The Energy Impact of Combined Solar Radiation/Infiltration/Conduction Effects in Walls and Attics

M. Liu, Ph.D

D.E. Claridge, Ph.D., P.E.
Member ASHRAE

ABSTRACT

Heat losses and gains through building components are calculated as the sum of terms due to conduction, solar radiation, and air infiltration. The current design methods ignore the interaction of air infiltration with either solar radiation or conduction in building components. Neglect of these interactions may account for a significant portion of the overestimated/underestimated house energy consumption.

This paper presents simplified, idealized models that simultaneously consider the influence and interactions of conduction, solar radiation, and infiltration as they affect heat transfer in attics and walls. The models are then used to simulate an idealized house, defined as fan depressurized in winter and fan pressurized in summer. The simulation results show that the idealized house can save 21% to 100% of the heating energy and 7% to 52% of the cooling energy due to opaque component loads under certain conditions compared to a "normal" house, where diffuse infiltration (air leaks through wall diffusely) is present only, and 38% to 100% of the heating energy and up to 33% of the cooling energy of opaque component loads over a "leak" house, where no air infiltration heat recovery is present under normal weather conditions.

INTRODUCTION

The heating/cooling load has been a key issue in building design since the 1970s, and the new design methods, such as the response factor method (Stephenson and Mitalas 1967), were developed to treat the dynamic characteristics of a building. These new methods produce dramatically lower design load estimates for heating and cooling, and the resulting more accurate equipment sizing has significantly improved HVAC efficiency. However, all the design methods assume that solar radiation, conduction, and air infiltration behave independently. This unrealistic assumption can cause substantial error in the estimation of design load and annual energy consumption.

The interaction of infiltration and conduction has been investigated by a number of researchers. Bursey and Green (1970) measured total energy consumption of double-frame windows when both infiltration and conduction were present and found that the actual load is only 80% of the calculated value. Guo and Liu (1985) developed a mathematical model of double windows, tested it experimentally, and found that the actual load is about 10% to 30% less than the calculated value. Anderlind (1985) and Kohonen et al. (1987) separately proposed combined conduction and air infiltration models of the wall. They claimed that air infiltration can recover 40% to 50% of the air infiltration energy consumption. Andersson and Wadmark (1987) tested an "optimum" ceiling based on the same principles and claimed that ceiling energy consumption can be recovered by organizing airflow. Recently, Claridge and Bhattacharyya (1989, 1990) measured up to 80% air infiltration energy recovery in an indoor test cell and a frame wall. Liu and Claridge (1992a, 1992b) investigated the dynamic properties of air infiltration in an indoor cell and the energy recovery of infiltration in an outdoor test cell with similar results. They also found that infiltration enhances heat recovery in winter by carrying more solar radiant energy into a cell, and exfiltration enhances heat recovery in summer by rejecting solar radiant energy to the outside. However, no theoretical model includes this solar factor.

This paper describes the development of combined solar, air infiltration, and conduction models for ideal diffuse attics and walls, gives numerical results from the models, and presents an application showing the potential energy savings that could result from "optimized" air infiltration in houses.

COMBINED MODELS

The ideal diffuse wall and attic are defined as uniform airflow through the wall and ceiling with both the solid material and air having the same temperature at any position. In order to make a simple analysis, a wall or attic is separated into two subsystems: the "outside" system (physically from outside air to the outside surface of the wall or to the attic air) and the base system (physically from the outside surface of the wall or attic air to room air).

The temperature distribution within a base system, where a constant air infiltration rate m ($kg/m^2 \cdot s$)—defined as positive for infiltration, negative for exfiltration—flows through the wall, can be expressed by Equation 1 under steady-state conditions (see Appendix A).

Mingsheng Liu is a research associate and **David E. Claridge** is an associate professor in the Energy Systems Laboratory, Texas A&M University, College Station.

$$\frac{T - T_w}{T_r - T_w} = \frac{1 - \exp(\alpha)}{1 - \exp(\alpha_w)} \quad (1)$$

where

T = temperature at resistance R,
T_w = outside surface temperature of base system,
T_r = room air temperature,
α = mC_pR,
α_w = mC_pR_w,
R = heat resistance, and
R_w = resistance from outside surface to room air.

According to the Fourier law of heat conduction, the total heat loss is

$$Q = (T_r - T_w)\frac{mC_p \exp(\alpha_w)}{1 - \exp(\alpha_w 0)} . \quad (2)$$

The overall/apparent heat transfer coefficient then is calculated by

$$UA_a = \frac{Q}{T_r - T_a} = (1-\theta)\frac{mC_p \exp(\alpha_w)}{1-\exp(\alpha_w)} = (1-\theta)\frac{\phi}{R_w} , \quad (3)$$

where

$$\theta = \frac{T_w - T_a}{T_r - T_a}, \quad (4)$$

$$\phi = \frac{\alpha_w \exp(\alpha_w)}{1 - \exp(\alpha_w)}. \quad (5)$$

However, the designed heat loss under the same conditions is calculated by

$$Q_d = \begin{cases} (\frac{1}{R_0} + mC_p)(T_r - T_a) - I\frac{R_{b0}}{R_0} & \text{Infiltration} \\ \frac{1}{R_0}(T_r - T_a) - I\frac{R_{b0}}{R_0} & \text{Exfiltration} \end{cases} \quad (6)$$

The apparent design heat transfer coefficient, then, is

$$UA_d = \begin{cases} \frac{1}{R_0} + mC_p - \beta\psi & \text{Infiltration} \\ \frac{1}{R_0} - \beta\psi & \text{Exfiltration} \end{cases} , \quad (7)$$

where

$$\psi = \frac{I}{T_r - T_a}, \quad (8)$$

$$\beta = \frac{R_w}{R_{b0}}. \quad (9)$$

Since current design methods do not consider the interaction of solar radiation, conduction, and air infiltration, Q and Q_d are different. Any difference between Q and Q_d is called air infiltration heat recovery, which can be expressed as a portion of designed air infiltration energy consumption or a portion of designed total energy consumption.

$$\varepsilon = \frac{Q_d - Q}{mC_p(T_r - T_a)} = \frac{UA_d - UA_a}{mC_p}, \quad (10)$$

$$\beta_e = \frac{Q_d - Q}{Q_d}. \quad (11)$$

ε is called the infiltration heat exchange effectiveness (IHEE) because it simulates a heat exchanger; β_e is called the total energy saving ratio; ψ is called the solar indicator, which equals the ratio of the absorbed solar intensity to the temperature difference between the room and outside; it has a positive value in winter and a negative value in summer. β is the resistance ratio.

Equations 10 and 11 apply to both walls and attics because it is presumed that the outside surface temperature is known. Sequentially, the model combines the "outside" system with the base system to find the nondimensional temperature (θ).

The schematic of the heat transfer process of walls is shown in Figure 1. The wall sustains constant solar radiation, I (W/m^2); airflow, m (kg/m^2·s); and temperature difference, $T_r - T_a$. The control surface of the system is shown in the figure with the dashed line. From the energy balance equation of the wall, the dimensionless surface temperature can be deduced as (see Appendix B)

$$\theta = \frac{\alpha_w + \phi - \psi R_{bo}}{\phi - \beta}. \quad (12)$$

The schematics of attic models are shown in Figure 2. The attic is assumed to sustain a constant cross ventilation, m_c (kg/m^2·s); infiltration/exfiltration, m, through the ceiling (kg/m^2·s), a temperature difference of $T_r - T_o$; and absorbed solar radiation, I. R_w is taken as the resistance between attic air and room air.

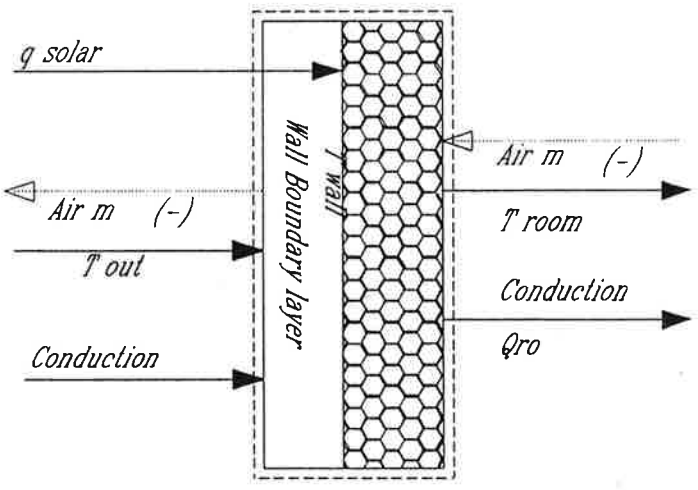

Figure 1 *Schematic of heat transfer process of the wall.*

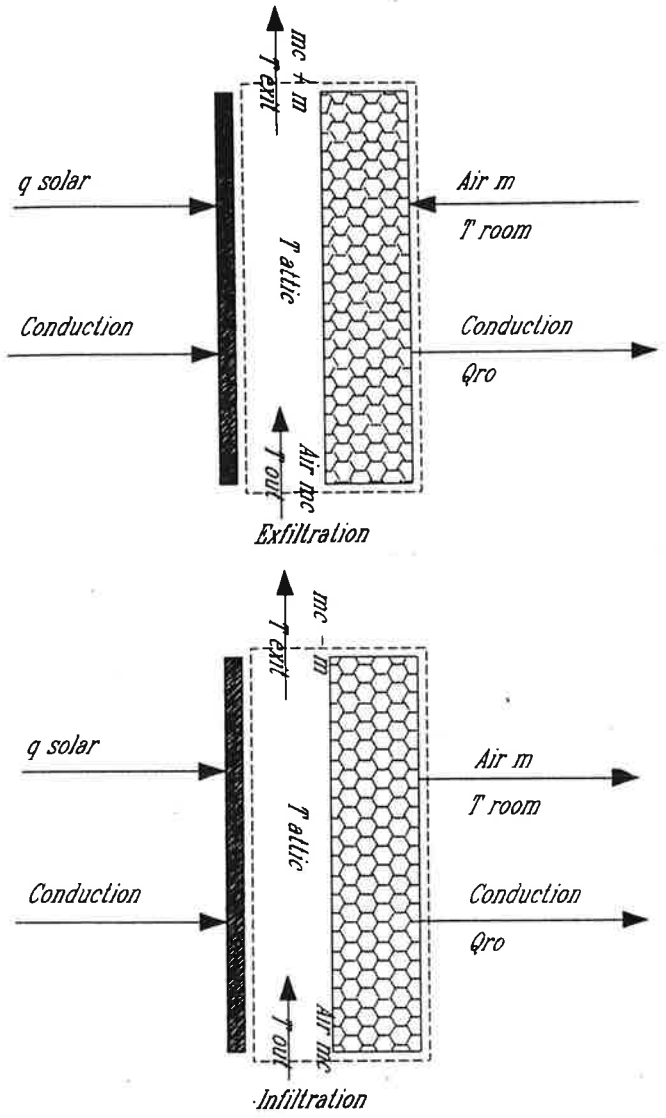

Figure 2 Schematic of attic heat transfer process.

Attic model *I* assumes that the cross-ventilation rate $m_c = 0$. Under this condition, the nondimensional attic air temperature is (see Appendix C)

$$\theta = \begin{cases} \dfrac{\phi - \psi\beta R_{bo} + \alpha_w}{\phi - \beta} & \text{Infiltration} \\ \dfrac{\phi - \psi\beta R_{bo} + \alpha_w}{\phi - \beta + \alpha_w} & \text{Exfiltration} \end{cases} \quad (13)$$

Attic model II assumes no infiltration/exfiltration present; under this condition, the nondimensional attic air temperature is (see Appendix D)

$$\theta = \frac{1 + \psi\beta R_{b0}}{1 + \beta + 2\alpha_c}. \quad (14)$$

Attic model III assumes that both infiltration/exfiltration and cross ventilation are present. Under these conditions, the attic air temperature is expressed as (see Appendix E)

$$\theta = \frac{\phi + \alpha_w - \psi\beta R_{b0}}{\phi + 2\alpha_w - \beta - \alpha_c} \quad (15)$$

where

$$\beta = \frac{R_w}{R_1}, \quad (16)$$

$$\theta = \frac{T_{attic} - T_a}{T_r - T_a}, \quad (17)$$

$$\alpha_c = m_c C_p R_2. \quad (18)$$

The analysis shows that the combined energy consumption and infiltration heat recovery can be expressed by the solar indicator (ψ), the nondimensional airflow rate (α), the resistance ratio (β), and the boundary layer resistance (R_{bo}). These ratio parameters make it possible to obtain general idealized results with limited simulation calculations.

SIMULATION AND NUMERICAL RESULTS

The simulation calculations have been carried out on a typical wall and attic that have the following thermal parameters:

- R_{bo} = 0.05 (°C·m²/W), heat resistance of outside boundary layer;
- R_w = 2(°C·m²/W), heat resistance from outside surface of the wall to room air;
- R_1 = 0.15(°C·m²/W), heat resistance from outside to attic air (including roof and two surface coefficients);
- R_w = 3(°C·m²/W), heat resistance from attic to room air for ceiling.

The possible ranges of daily average solar radiation, outside temperature variation, and air infiltration require the following combined parameter ranges in simulations:

- ψ = solar indicator −100 to 40 (W/m²·°C), negative values indicate cooling and positive values indicate heating;
- α = nondimensional airflow rate −1 to 1, negative values indicate exfiltration, positive values indicate infiltration.

The IHEE values of the diffuse wall are shown in Figure 3 as a function of solar indicator (ψ) and nondimensional airflow rate (α_w). In the heating season, IHEE increases as solar radiation increases for infiltration but decreases for exfiltration because infiltration carries more solar radiant energy inside and exfiltration rejects solar radiant energy to the outside. In the cooling season, IHEE increases as solar radiation increases for exfiltration but decreases for infiltration because exfiltration rejects more solar radiant energy to the outside and reduces the cooling load. With the ranges of the solar indicator and airflow rate simulated, IHEE can be up to 2.8 and as low as −2.3.

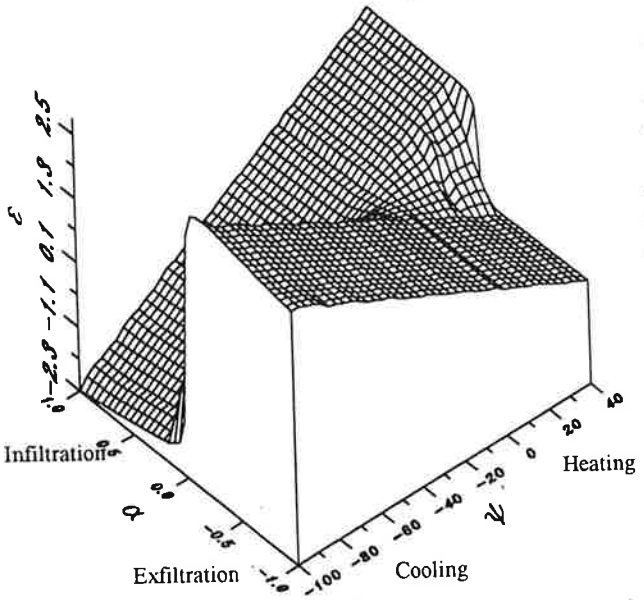

Figure 3 *IHEE of combined diffuse wall model—ε = IHEE, ψ = solar indicator (W/m²·°C), α = nondimensional airflow rate.*

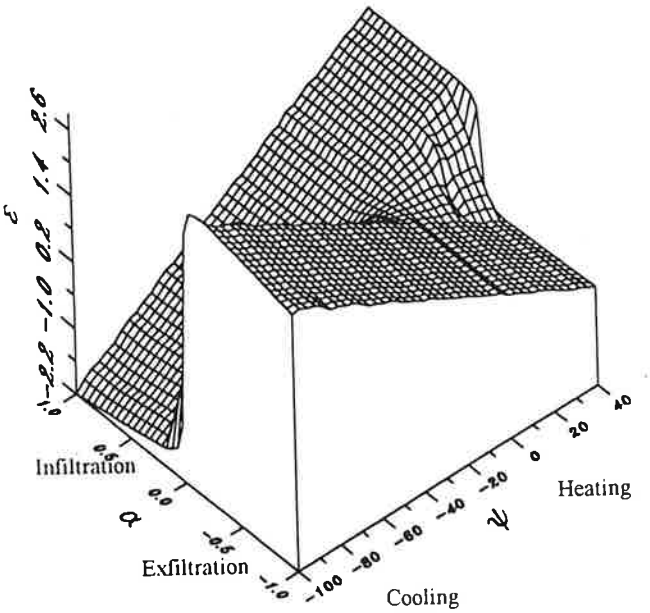

Figure 4 *IHEE of combined model for attic I—ε = IHEE, ψ = solar indicator (W/m²·°C), α = nondimensional airflow rate (diffuse infiltration/exfiltration only).*

For a nondimensional airflow rate of 0.6 and normal weather conditions (Houston area) corresponding to a solar indicator of 20 W/m²·K for winter, IHEE is 0.97 for heating. For a nondimensional airflow rate, −0.6, and solar indicator −40 W/m²·K for summer conditions, IHEE is 1.31 for cooling. However, if infiltration is used for summer and exfiltration is used for winter, the IHEE changes from 0.97 to 0.02 for heating and from 1.31 to −0.59 for cooling. These numbers show that energy saving might be achieved by organizing the airflow; normal airflow can increase the cooling energy consumption if infiltration is predominant on sunny walls and the roof.

The IHEEs of attic model I (no cross ventilation) are shown in Figure 4. The results are qualitatively similar to those of Figure 3. With the weather and airflow rate defined above, IHEE is 0.95 for heating with infiltration and 1.34 for cooling with exfiltration.

Attic model II (cross ventilation only) is a special case because there is no infiltration present. The energy-saving ratios (β_e) are given in Figure 5. The results show that the energy-saving ratio decreases for heating with increases in cross ventilation and solar radiation, but it increases for cooling with increases in cross ventilation and solar radiation. Under the normal conditions defined earlier but with a cross-ventilation rate (α_c) of 5, the heating energy consumption of the attic could be doubled, and cooling energy could be reduced about 17% by cross ventilation. Obviously, cross ventilation of the attic should be avoided in winter to save energy.

The IHEEs of attic model III (cross-ventilation rate α_c = 5) are shown in Figure 6. The results show that the profile of the IHEE is very different from those of Figures 3 and 4, where IHEE increases sharply with solar radiation in summer when the airflow rate (α_w) is small but decreases sharply with solar radiation in winter when the airflow rate (α_w) is small. This behavior indicates that cross ventilation is the dominant factor when air infiltration (α_w) is low. Under the normal weather conditions defined earlier, IHEE

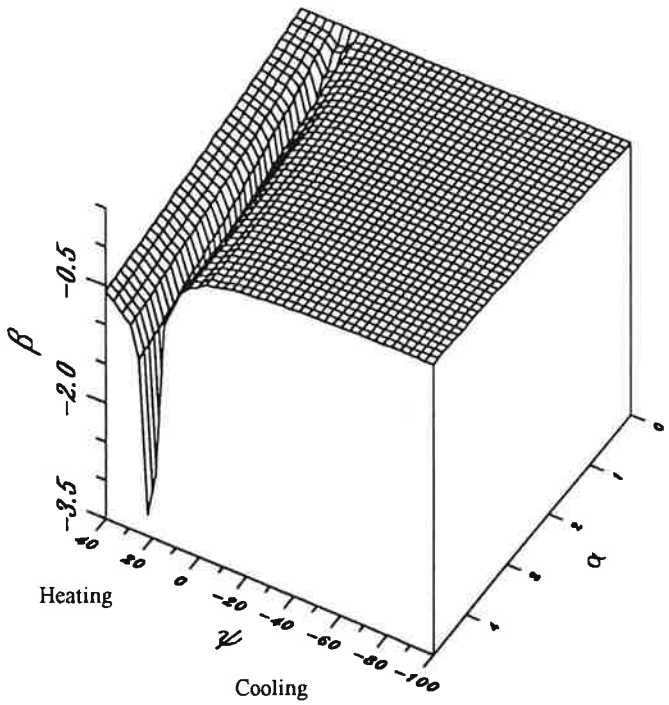

Figure 5 *Energy-saving ratio of attic II—β = energy-saving ratio, ψ = solar indicator (W/m²·°C), α = nondimensional airflow rate (cross ventilation only).*

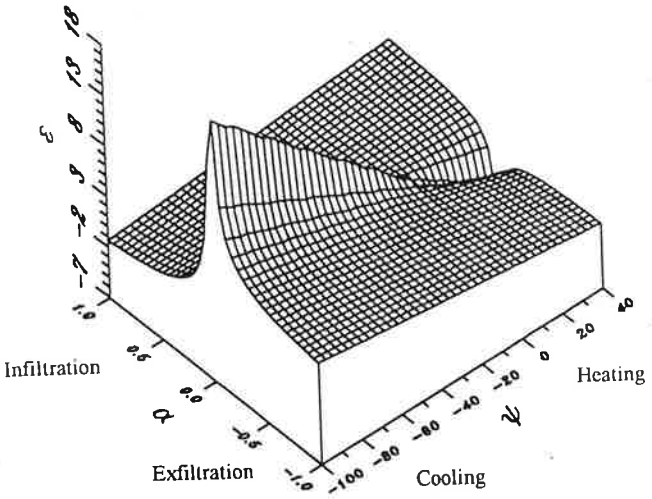

Figure 6 *IHEE of combined model for attic III (α_c = 5)—ε = IHEE, ψ = solar indicator ($W/m^2 \cdot °C$), α = nondimensional airflow rate (both diffuse infiltration/exfiltration and cross ventilation present).*

is about 0.66 for heating with infiltration and 1.75 for cooling with exfiltration. The numbers show that attic III consumes 30% more heating energy and 40% less cooling energy than attic I.

APPLICATION

The model analysis shows substantial energy saving might be obtained by using the proper location for infiltration and exfiltration. A simplified house model is chosen to demonstrate the energy-saving effects. The fundamental thermal parameters of the house are summarized in Table 1.

The "idealized" house model is defined as a house that is depressurized in winter and pressurized in summer by a fan and has uniform infiltration. "Uniform infiltration" means that both the opaque walls and ceilings have identical nondimensional airflow rates. It is further assumed that the total airflow through the ceiling is the same as that through windows. No heat recovery is considered for windows.

In the "normal" house model, air leaks in through half the wall and leaks out through the other half, and the ceiling has infiltration in summer and exfiltration in winter because of the thermal stack effect. Again, both the opaque walls and the ceiling have the same nondimensional airflow rate. No combined effect is considered for windows and doors.

The "designed" house model calculates total energy consumption as the sum of the conduction and air infiltration energy consumption where noninteraction is considered. This model essentially represents a "leak" house where no air infiltration heat recovery actually occurs.

The simulation assumed the attic has no cross ventilation, and the solar radiation on all walls, regardless of orientation, is two-thirds of the solar radiation on the roof. The simulation covered a nondimensional airflow rate range from 0 to 1 with a step of 0.05 and a roof solar indicator range from 0 to 40 for winter and −100 to 0 for summer with a step of 2. The outputs of the simulation are the energy savings ratios of the idealized house vs. the normal house (*I*/*N*),

$$\left[\frac{Q_n - Q_i}{Q_n}\right],$$

the idealized house and the designed house (*I*/*D*),

$$\left[\frac{Q_d - Q_i}{Q_d}\right],$$

and the normal house and the designed house (*N*/*D*),

$$\left[\frac{Q_d - Q_n}{Q_d}\right].$$

The simulation did not include the window conduction and radiation load and the floor load.

A comparison of energy consumption for the idealized and normal house models is given in Figure 7. The results show that the energy-saving ratio of the idealized house varies from −0.15 to greater than 2 in winter and from −0.15 to 0.52 in summer depending on the solar indicators and nondimensional airflow rates. When the absolute value of the solar indicator is greater than 10, the energy-saving ratio is positive. If the solar indicator is 20 for winter and −40 for summer, then the idealized house model can save from 21% to 35% of the heating energy and from 7% to 31% of the cooling energy when the nondimensional airflow varies from 0.2 to 1. These numbers demonstrate the potential energy savings that could result from organizing the airflow through the house envelope. If the house can be operated as a "normal" house when the absolute value of the solar indicator is less than 10, the seasonal energy savings of the house will increase.

TABLE 1
Summary of Thermal and Associated Parameters for the House Model

External dimension of house	12×15×2.4 m (39×49×8 ft)
Area of ceiling	180 m^2 (1938 ft^2)
Area of opaque walls	104 m^2 (1116 ft^2)
Area of windows	26 m^2 (279 ft^2)
R_w for walls	2 m^2K/W (11 $ft^2h°F/Btu$)
R_w for ceiling	3.5 m^2K/W (20 $ft^2h°F/Btu$)
R_1 for ceiling	0.15 m^2K/W (0.85 $ft^2h°F/Btu$)
R_{h0}	0.05 m^2K/W (0.28 $ft^2h°F/Btu$)

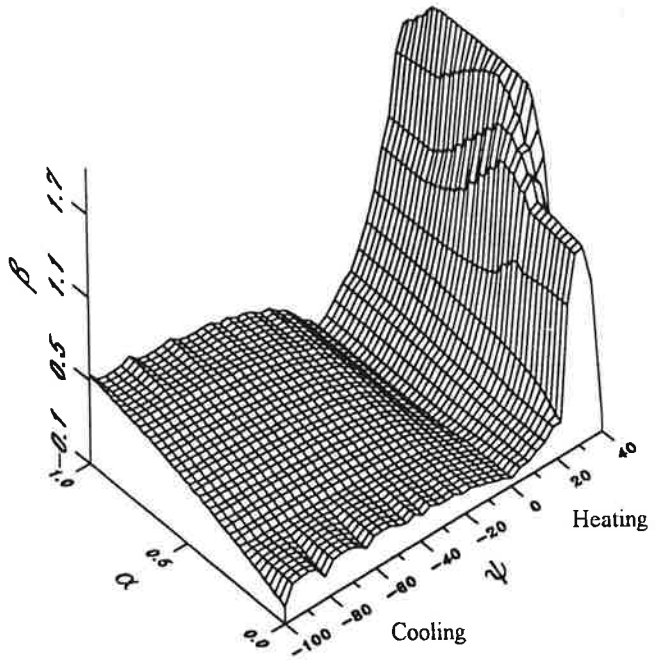

Figure 7 *Energy-saving ratio of the idealized to normal house models—β = energy-saving ratio, ψ = solar indicator (W/m^2·°C), α = nondimensional airflow rate.*

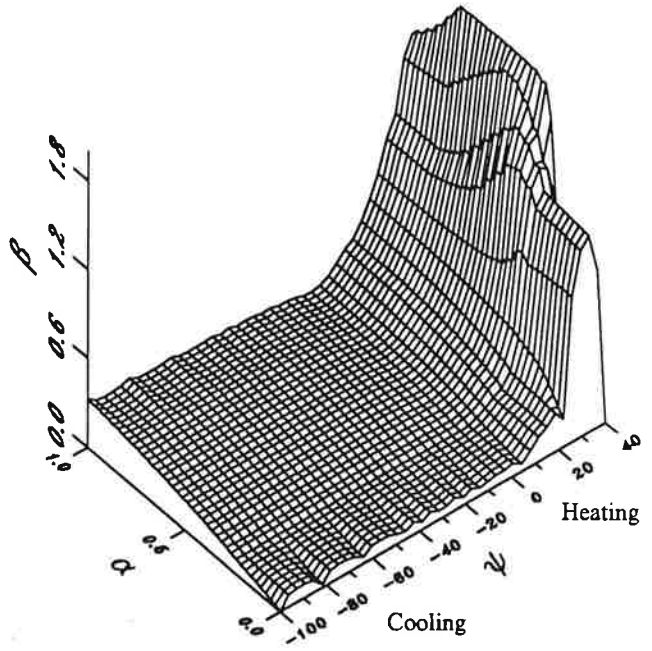

Figure 8 *Energy-saving ratio of the idealized to designed house models—β = energy-saving ratio, ψ = solar indicator (W/m^2·°C), α = nondimensional airflow rate.*

A comparison of energy consumption of the idealized and designed house models is given in Figure 8. The results show that the saving ratio varies from 0 to greater than 2 in winter and from 0 to 0.33 in summer. The energy-saving ratio increases with both solar radiation and airflow. If the solar indicator is 20 in winter and −40 in summer, the heating energy-saving ratio varies from 0.38 to 0.52 and the cooling energy-saving ratio varies from 0.09 to 0.27 when the nondimensional airflow varies from 0.2 to 1. These numbers demonstrate the energy-savings potential of an idealized house compared to design calculation or over a poorly designed house where no heat recovery is present.

A comparison of the "normal" and "designed" house models is given in Figure 9. The results show that the energy-saving ratio varies from 0 to 0.91 for heating and from −0.40 to 0.28 for cooling. If the solar indicator is 20 in winter and −40 in summer, the heating energy-savings ratio varies from 0.21 to 0.26 and the cooling energy-saving ratio varies from −0.05 to −0.16 when the nondimensional airflow varies from 0.2 to 1. These numbers demonstrate that design calculations might overestimate heating energy consumption by 21% to 26% and underestimate cooling energy consumption by 5% to 16%.

DISCUSSION AND CONCLUSION

The models used in the paper are simplified and idealized in order to understand and investigate the maximum potential of air infiltration heat recovery in house components and houses. The concept of diffuse leakage may represent uniform infiltration for porous insulation; however, air infiltration heat recovery effects for most walls are smaller than those for porous insulation; also, effects of circulation flow within walls are not considered. The idealized house model might represent seasonal average conditions for most houses; however, the actual condition of a house may be quite different from what is assumed in the model. Although the models used in the analysis are not complete, the results of the simulation still indicate the

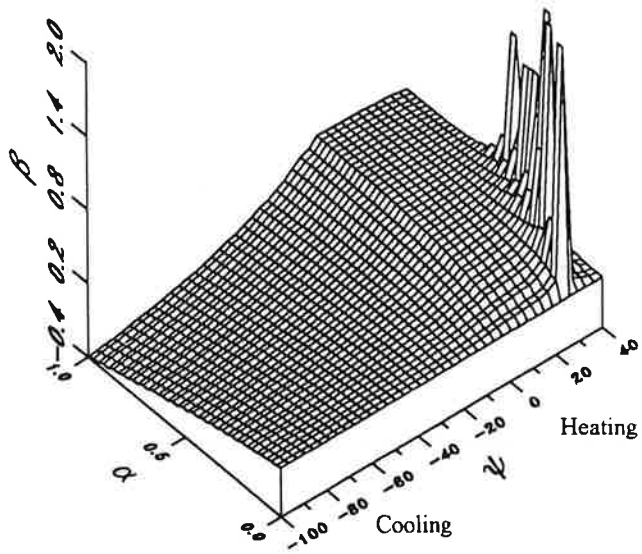

Figure 9 *Energy-saving ratio of the normal to designed house models—β = energy-saving ratio, ψ = solar indicator (W/m^2·°C), α = nondimensional airflow rate.*

approximate magnitude of the infiltration energy impact in general, and some helpful suggestion can be concluded from this work.

Air infiltration energy consumption is not only dependent on airflow rate and temperature difference between a room and the outside but is also dependent on airflow direction, solar radiation, and leakage configuration. The infiltration flow enhances heat recovery in winter by carrying more solar radiant energy into a room, and exfiltration enhances heat recovery by rejecting solar radiant energy to the outside in summer. Air infiltration heat recovery appears important for house energy conservation. Also, attic cross ventilation should be avoided for heating.

The simulations suggest that the idealized house can save from 2% to 32% heating energy and 25% to 31% cooling energy compared to the normal house, where diffuse infiltration dominates the air infiltration, and from 27% to 49% heating energy and 20% to 22% cooling energy compared to design calculations or a "leak" house, when the solar indicator is 20 in winter and −40 in summer and the nondimensional airflow rate is 0.6.

The overestimation of energy consumption with the design method is substantial. The simplified, idealized simulations show that the design method overestimated heating energy by 49% and cooling energy by 22% for the components modeled in the idealized house and heating energy by 26% in the normal house and underestimated cooling energy by 14% in the normal house.

The actual energy consumption of walls and houses can be either less than or greater than the designed values because of the impact of airflow direction on solar radiation. To utilize or maximize air infiltration heat recovery in walls, air infiltration must be organized; otherwise, the diffuse infiltration may actually cause more energy consumption. The infiltration flow model should be used in winter and the exfiltration flow model in summer.

The climate can be easily classified by the seasonal solar indicator; consequently, the seasonal IHEE or energy-saving ratio, β_e, can be estimated easily.

This analysis was based on simplified steady-state models, where neither the latent cooling load nor the load from windows, doors, and the ground was included. The extended models and seasonal dynamic simulation could be considered for future work. Infrared heat radiation, the attic heat exchange model, total house building energy consumption, and latent cooling energy consumption need to be better addressed.

NOMENCLATURE

C_p = specific heat of air (J/kg·°C)
I = solar radiation (W/m^2)
m = air infiltration rate (kg/m^2·s)
m_c = attic cross-ventilation rate (kg/m^2·s)
R = heat resistance (W/m^2·°C)$^{-1}$
R_0 = heat resistance of the wall (W/m^2·°C)$^{-1}$
R_1 = heat resistance from outside air to attic air (W/m^2·°C)$^{-1}$
R_{b0} = heat resistance of the outside boundary layer (W/m^2·°C)$^{-1}$
R_w = heat resistance from out-surface of the wall to room air or from attic air to room air (W/m^2·°C)$^{-1}$
T = temperature (°C)
T_a = outside temperature (°C)
T_{attic} = attic air temperature (°C)
T_r = room air temperature (°C)
T_w = outside surface temperature of the wall (°C)
UA_a = apparent heat transfer coefficient (W/m^2·°C)
UA_d = designed apparent heat transfer coefficient (W/m^2·°C)$^{-1}$
α = nondimensional airflow rate
β = resistance ratio
ε = infiltration heat exchange effectiveness
ψ = solar indicator (W/m^2·°C)
θ = nondimensional temperature

REFERENCES

Anderlind, G. 1985. Energy consumption due to air infiltration. *Proceedings of the 3rd ASHRAE/DOE/BTECC Conference on Thermal Performance of the Exterior Envelopes of Buildings*, Clearwater Beach, FL, pp. 201-208.

Andersson, K.A., and T. Wadmark. 1987. Use of ventilation and insulation in single family houses for thermal comfort, energy conservation and protection against moisture, dust and radon, the OPTIMA concept. *Proceedings of the 3rd International Congress on Building Energy Management ICBEM '87*, Lausanne, Switzerland, October, Vol. 3.

Bursey, T., and G.H. Green. 1970. Combined thermal and air leakage performance of double windows. *ASHAAE Transactions* 73: 215-226.

Claridge, D.E., and S. Bhattacharyya. 1989. The measured energy impact of "infiltration" in a test cell. *Proceedings of the Eleventh Annual ASME Solar Energy Conference*, San Diego, CA, April.

Claridge, D.E., and S. Bhattacharyya. 1990. The measured energy impact of "infiltration" in a test cell. *Journal of Solar Energy Engineering* 112: 132-139.

Guo, J., and M. Liu. 1985. The energy saving effect of double frame windows. *Proceedings of the CLIMA 2000 World Congress in Heating, Ventilating and Air-Conditioning*, Copenhagen, August, Vol. 2.

Liu, M., and D.E. Claridge. 1992a. The measured energy impact of infiltration under dynamic conditions. *Proceedings of Symposium on Improving Building Systems in Hot and Humid Climates.*

Liu, M., and D.E. Claridge. 1992b. The measured energy impact of infiltration in an outdoor test cell. *Proceedings of Symposium on Improving Building Systems in Hot and Humid Climates.*

Stephenson, D.G., and G.P. Mitalas. 1967. Cooling load calculations by thermal response method. *ASHRAE Transactions* 73(2).

APPENDIX A

A base part of an ideal diffuse wall or attic is shown in Figure A-1, where resistance R was chosen as the axis. This makes it possible to get a general differential equation for multilayer walls under steady-state conditions. Consequently, it simplifies the analysis substantially. The base system sustained an air infiltration, m (kg/m^2·s), defined as positive for infiltration, negative for exfiltration. The outside surface temperature and room temperature were represented by T_w and T_r, respectively. The heat resistance of the wall from the outside surface to room air was R_w. The conductive and air infiltration heat fluxes within the base system were generally expressed as

$$Q_c = -k\frac{dT}{dx} = -\frac{dT}{dR}, \tag{A1}$$

$$Q_a = mC_p(T - T_r), \tag{A2}$$

where

C_p = specific heat of air (J/kg·K),
m = airflow rate (kg/m^2·s),
T = temperature of the wall section at R,
R = heat resistance of the wall from outside to the position,
T_r = room temperature.

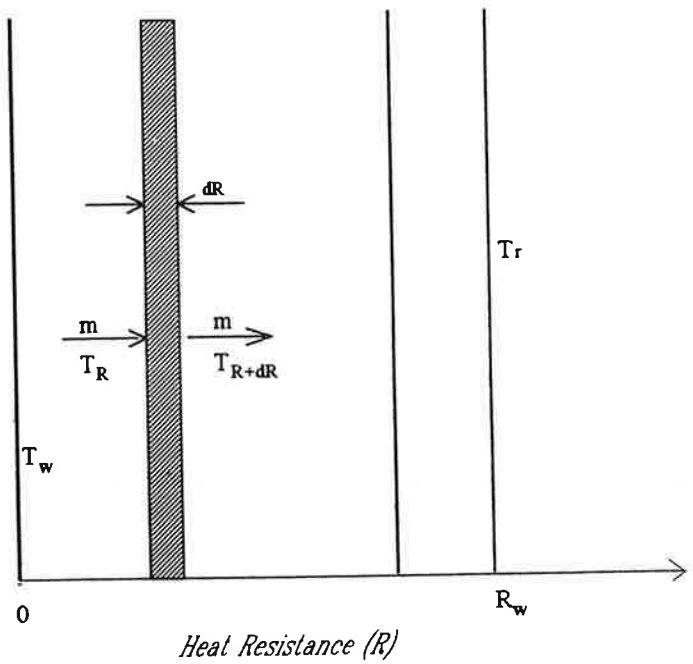

Figure A1 *Schematic of diffuse wall base system.*

The differential equation was established by balancing the energy fluxes of a finite element (dr) under steady-state conditions:

$$\frac{d^2T}{dR^2} - mC_p\frac{dT}{dR} = 0, \tag{A3}$$

$$T = T_w,\ R = 0, \qquad T = T_r,\ R = R_w. \tag{A4}$$

The solution of this equation is

$$\frac{T - T_w}{T_r - T_w} = \frac{1 - \exp(mC_pR)}{1 - \exp(mC_pR_w)}. \tag{A5}$$

The mC_pR_w was the ratio of maximum heat loss factors (mC_p and $1/R_w$) due to infiltration and conduction, respectively. It was called the nondimensional airflow rate and is expressed by α_w since the heat loss factor due to conduction was considered a constant for a wall. Similarly, the mC_pR was expressed as α. Introducing this convention into Equation A5, it then followed:

$$\frac{T - T_w}{T_r - T_w} = \frac{1 - \exp(\alpha)}{1 - \exp(\alpha_w)}. \tag{A6}$$

APPENDIX B

The schematic of the heat transfer process of the ideal diffuse wall is shown in Figure 1, where the outside surface boundary layer was treated as a separate layer because the solar radiation penetrated without resistance. The wall sustained a constant solar radiation, I (W/m^2); airflow rate, m (kg/m^2·s); and temperature difference, $T_r - T_a$. The control surface of the system is shown in the figure with a dashed line. The energy balance on the control volume led to the following equation:

$$\frac{T_a - T_w}{R_{b0}} + I - Q + mC_pT_a - mC_pT_r = 0. \tag{B1}$$

Dividing both sides of Equation B1 by $T_r - T_a$ and introducing Equation 2 into Equation B1, it then followed:

$$-\theta\frac{1}{R_{b0}} + \psi - (1 - \theta)\frac{\phi}{R_w} - mC_p = 0. \tag{B2}$$

Rearranging Equation (B2), the nondimensional temperature was then expressed as

$$\theta = \frac{\alpha_w + \phi - \psi R_w}{\phi - \beta}. \tag{B3}$$

APPENDIX C

Attic I, defined as that attic without cross ventilation, was idealized as a two-layer system, shown in Figure 2. To take the control system as the dashed line shown in Figure

2 (infiltration), the energy balance equation for the infiltration case is

$$mC_pT_a + I\frac{R_{b0}}{R_1} + (T_a - T_{attic})\frac{1}{R_1} = mC_pT_r + Q \quad \text{(C1)}$$

where

m = infiltration rate through the ceiling (kg/m^2·s),
R_1 = heat resistance of the outer layer (shingle) (W/m^2·K),
T_{attic} = attic temperature (°C).

Combining Equations 2 and C1, the nondimensional temperature then follows:

$$\theta = \frac{\phi - \psi\beta R_{b0} + \alpha_w}{\phi - \beta} \quad \text{(C2)}$$

where

$$\beta = \frac{R_w}{R_1}, \quad \text{(C3)}$$

$$\theta = \frac{T_{attic} - T_a}{T_r - T_a}, \quad \text{(C4)}$$

where

R_w = heat resistance from attic air to room air.

The only difference between infiltration and exfiltration for attic I was that the air leakage temperature at the outside surface of the roof system was T_{attic} rather than T_a (see Figure 2 exfiltration). Thus the energy balance equation was

$$mC_pT_{attic} + I\frac{R_{b0}}{R_1} + (T_a - T_{attic})\frac{1}{R_1} = mC_pT_r + Q. \quad \text{(C5)}$$

The nondimensional temperature can be deduced by a procedure similar to the above:

$$\theta = \frac{\phi + \alpha_w - \psi\beta R_{b0}}{\phi + \alpha_w - \beta}. \quad \text{(C6)}$$

APPENDIX D

Attic model II sustained cross ventilation only. The energy balance equation on the control volume was expressed as

$$(T_a - T_{attic})\frac{1}{R_1} + (T_r - T_{attic})\frac{1}{R_w} + I\frac{R_{b0}}{R_1} + m_cC_pT_a - m_cC_pT_{exit} = 0 \quad \text{(D1)}$$

where

T_{exit} = air temperature when the air leaves the attic,
m_c = cross-ventilation rate (kg/m^2·s).

The attic temperature was defined as

$$T_{attic} = \frac{1}{2}(T_{exit} + T_a). \quad \text{(D2)}$$

The nondimensional attic temperature was obtained by combining Equations 2, D1, and D2:

$$\theta = \frac{1 + \psi\beta R_{b0}}{1 + \beta + 2\alpha_c} \quad \text{(D3)}$$

where

$$\alpha_c = m_cC_pR_2. \quad \text{(D4)}$$

APPENDIX E

Attic model III has both infiltration and cross ventilation. The energy balance equation was established according to the schematic figure:

$$(T_a - T_{attic})\frac{1}{R_1} + m_cC_pT_a + I\frac{R_{b0}}{R_1} - mC_pT_r - Q - (m_c - m)C_pT_{exit} = 0 \quad \text{(E1)}$$

where

$$T_{attic} = \frac{1}{2}(T_a + T_{exit}). \quad \text{(E2)}$$

The nondimensional attic temperature was deduced from Equations 2, E1, and E2 as

$$\theta = \frac{\phi + \alpha_w - \psi\beta R_{b0}}{\phi + 2\alpha_w - \beta - \alpha_c} \quad \text{(E3)}$$

where

$$\alpha_c = m_cC_pR_w. \quad \text{(E4)}$$